Physical and Numerical Modeling of the mixing time in the IronArc pilot plant

*Kristofer Bölke[1], Mikael Ersson[1], and Pär G. Jönsson[1]

[1] KTH-Royal Institute of Technology, SE-100 44 Stockholm, Sweden

*Corresponding: bolke@kth.se
Mikael Ersson: bergsman@kth.se
Pär Jönsson: parj@kth.se

Abstract

IronArc is a new emerging process technology for pig iron production. The process exists at a pilot plant scale, but a long-term goal is to scale up the process to an industrial scale to become an alternative process to the current pig iron production processes. One of the key concepts in the process is the use of a plasma generator to obtain a submerged gas injection. This injected gas creates stirring, heating and is also used as a reducing agent. The production rate of the IronArc process is dependent on the stirring and in turn on the mixing time, which is the focus of this study. First, the mixing time was determined in a physical acrylic plastic 1:3 scale model, by measuring the concentration of a tracer at specific measurement points. Thereafter, the mixing time was determined numerically for both the air-water case as well as the gas-slag case. This was done by using the Eulerian multiphase model to describe the gas and liquid phases and a species transport model to account for the tracer. The results showed that it was possible to determine the mixing time when comparing the physical water model experiments with the numerical simulations. The difference with respect to the 95% homogenization degree of the tracer in the bath between the two cases was only 1.3%, which is considered to be very good. Moreover, the mixing times for the experiments and numerical simulations were 7.5s and 7.6s, respectively. Furthermore, the simulation of the pilot plant gas-slag reduction degree for a 95% homogenization degree was found to be 6.5s. These results were in line with the results from earlier industrials mixing time trials, which showed that the mixing times were equal to or lower than 10 seconds.

Keywords: Reduction, Iron ore, IronArc pilot plant, Mixing time, CFD modeling.

1. Introduction

Numerical modeling is a useful tool to study phenomena that are difficult to investigate experimentally or to study upscaling of different processes in the steel and iron industry. More specifically, it is a tool that is beneficial both from an economic standpoint and for the development of new processes. The IronArc is a new emerging process for pig iron production, which is developed by ScanArc in Hofors, Sweden. The process exists at a pilot plant scale, but a long-term goal is to scale up the process to an industrial scale so that it can become an alternative process to the current pig iron production processes. Preliminary calculations have shown that the use of the IronArc process will reduce both the CO_2 emissions and energy usage compared to existing technologies [1].

A schematic figure of the IronArc pilot plant process can be seen in figure 1. The process uses submerged gas injection through a plasma generator that is located at the bottom part of the cylindrical wall of the reactor. Magnetite and hematite are the charged materials in the reactor and the gas is a mixture of air and LPG (Liquefied Petroleum Gas). The injected gas has a temperature of around 3500-4000°C, which will melt the charged material, create stirring in the reactor as well as reduce the hematite and magnetite to wüstite. More specifically, the following reactions appear during the reduction of the iron oxides to pure pig iron:

$$Fe_3O_4(s) + CO(g) = 3FeO(l) + 2CO_2(g) \quad (1)$$

$$Fe_3O_4(s) + H_2(g) = 3FeO(l) + H_2O(g) \quad (2)$$

$$Fe_2O_3(s) + CO(g) = 2FeO(l) + CO_2(g) \quad (3)$$

$$Fe_2O_3(s) + H_2(g) = 2FeO(l) + H_2O(g) \quad (4)$$

$$FeO(s) + C(s) = Fe(l) + CO(g) \quad (5)$$

The created CO and H_2 from the heated air and LPG reduce the magnetite and hematite to wüstite, equations (1) – (4). Then, carbon is used as a reducing agent for the final reduction from wüstite to pig iron, as seen in equation (5). Due to that the injected gas will be used for melting, heating and to create stirring in the bath as well as be used as a reducing agent, it is of large importance to determine the distribution of the injected bubbles and the mixing in the bath. Based on these data it is possible to determine the production efficiency of the process, which is an important parameter for a future upscaling of the process.

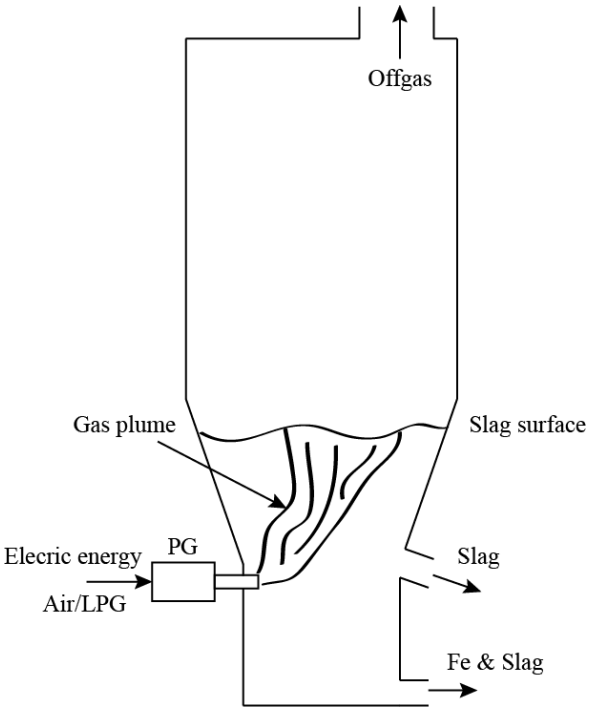

Figure 1: A schematic figure of the IronArc pilot plant process.

This IronArc process is a new technology, which has been investigated in three earlier studies. In the first study, the mixing time and penetration depth were investigated based on physical water model experiments using in a 1/3 scale acrylic plastic model [2]. The results indicated that the mixing was fast and that the average mixing time was 7.6 seconds, when averaging over the 6 trials performed to obtain a 95 % homogenization degree of the tracer in the bath and when using one gas inlet. Also, when using one inlet a pending motion of the surface was clearly seen. However, the mixing times were increased when using three inlets instead of one inlet. Specifically, there were a 15.8% and a 17.6% increase in the mixing times for the 95% and 99% homogenization degrees for the case when using three inlets and using the same flow rate as for the one inlet case. The explanation for this was a calmer surface, which resulted in a reduced pending motion in the radial direction and hence an increased mixing time. In the second study [3], the penetration depth of the injected gas was investigated numerically. The results showed that the gas reaches to approximately the center of the bottom part of the cylindrical reactor. This penetration depth results in an efficient usage and distribution of the gas in the slag. This, in turn, enhances the mixing and enables that the bubbles reach a large part of the slag. In the third study of the IronArc process [4], the mixing time was investigated in the pilot plant by taking continuous samples of the slag after a tracer had been added. Thereafter, the tracer content in the different slag samples was determined. The results showed that the mixing time was approximately 8 seconds (for sure below 10 seconds) when the tracer was homogenized in the slag. Based on the slag composition a thermodynamic

evaluation was done, which indicated that the slag was in a liquid state for the current process conditions.

The mixing time has been determined and used as a measurement of the stirring efficiency for several converters in the steel industry. Small scale water modeling for side blowing converters has extensively been used to determine the mixing [5-14]. Among others, Visuri et al.[5] studied the mixing time of a 1:9 scale physical model of the AOD process reduction step. The mixing time was determined based on pH measurements. Furthermore, Samuelsson et al.[6] investigated the mixing time of a 1:4.6 scaled of a 120 t AOD vessel with the aim to increase the production capacity by using an oblong converter. Also, Ternstedt et al.[7] used physical modelling to investigate the mixing time in the AOD process. Their results showed that the mixing time is dependent on the gas flow rate and the diameter of the converter. However, the bath height was found not affect the mixing to a large extent.

The mixing time has also been determined based on mathematical modeling [15-17]. Zhou et al.[15] investigated the mixing in a 1:6 scale 30 ton converter vessel by suing both mathematical and physical modelling. The difference between the predictions and measurements were found to be only 2.8%. In addition, Li et al. [16] studied the mixing time of a top and bottom blown converter by using mathematical modeling. Specifically, the focus was on studying the effect of the number of bottom blowing tuyeres and their locations on the mixing time. Chibwe et al. [17] studied the mixing efficiency in a Pierce-Smith converter by numerical modeling. The effect of the slag level thickness on the mixing time was investigated numerically as well as experimentally. It was shown that an increased slag thickness resulted in a shorter mixing time.

The goal with the present work was to determine the mixing time was numerically, for both a 1/3 scale acrylic plastic model as well as for a full-scale pilot plant process. The numerical model predictions were compared to the experimentally determined mixing times. As mentioned earlier, this information is of high importance since the IronArc process is completely dependent on a good stirring and mixing. Furthermore, this information can provide essential information for a future upscaling of the process, to an industrial scale.

2. Physical model experimental method

A 1:3 scale acrylic plastic model of the IronArc pilot plant process was designed for the experiments. All the lengths in the model are 1/3 of the reactor lengths in order to maintain a geometric similarity between the model and the pilot plant reactor. The dynamic similarity between the model setup and the pilot plant setup was realized by using the modified Froude number, which had similar values in the model and pilot plant. This dimensionless number is defined as the ratio of inertial forces to the buoyancy forces (equation 6):

$$N_{Fr'} = \frac{\rho_g u_0^2}{g \rho_l d_0} \quad (6)$$

where $N_{Fr'}$ is the modified Froude number, ρ_g (kg) and ρ_l (kg) are the density for the gas and the liquid, respectively. The parameter u_0 (m/s) is the velocity of the gas at the inlet and g (ms^{-2}) is the gravitational acceleration constant. Furthermore, d_0 (m) is the characteristic length of the system, which represents the diameter of the reactor. The scaling of the flow rate was based on equation (7). This is frequently used for scaling of flow rates when the modified Froude number is used as the similarity criteria. [6,7,18]

$$Q_m = Q_R \lambda^{2.5} \quad (7)$$

where Q_m (m^3s^{-1}) is the flowrate for the downscaled model, Q_R (m^3s^{-1}) is the flowrate in the pilot plant process, and λ is the scale factor having a value of 1/3 in the current setup. The diameter of the inlet was determined from equation (8), when both the velocity and flow rate at the inlet were given:

$$Q = \frac{u \pi d^2}{4} \quad (8)$$

The mixing time is defined as the time it takes to homogenize a liquid content in a tank, to a chosen degree of homogenization. More specifically, the mixing time, in this case was defined as the time for the liquid bath to reach a homogenization degree of 95%. This degree of homogenization of the final tracer content was measured after a tracer element had been added to the liquid bath. Specifically, this was done until the uniformity value, H, had reached values between 0.95 and 1.05. In addition, the time to reach a 99% homogenization degree in the bath was determined. The definition of H is given in Equation (9):

$$H = \frac{C(t)}{C_f} \quad (9)$$

where H is the degree of homogenization, $C(t)$ is the concentration at time t, and C_f is the final concentration value in the water when the tracer has been completely homogenized in the water. The mean value of the tracer measurements at the different probe positions is applied to obtain the mixing time as has been described in previous research [15, 19, 20].

In the experiments, water was used as the liquid and compressed air as the gas. The experimental set up for determining the mixing time can be seen in figure 2. The compressed air was blown in to the water through a nozzle that was connected to the wall of the model. To control the flow rate, a flow control meter was connected to the gas supply before it was injected into the bath through the nozzle. At the beginning of an experiment, a tracer solution consisting of a 20wt% NaCl solution was added to the bath. Thereafter, the conductivity in the water was measured by using two conductivity probes. The probes used for conductivity measurement were equipped with temperature compensation, which means that the measured conductivity corresponds to a value at the reference temperature of room temperature (25 °C). Logging of the conductivity data was done every second during the entire time of an experiment. The time required for the probes to measure a concentration reaching a 95% homogenization degree of the final concentration in the liquid bath was determined as the mixing time. The sodium chloride solution tracer was added to the water when the flow field was fully developed, since the blowing were done for a time that was several times longer than the mixing time for this process. All experimental parameters and conditions are given in table 1.

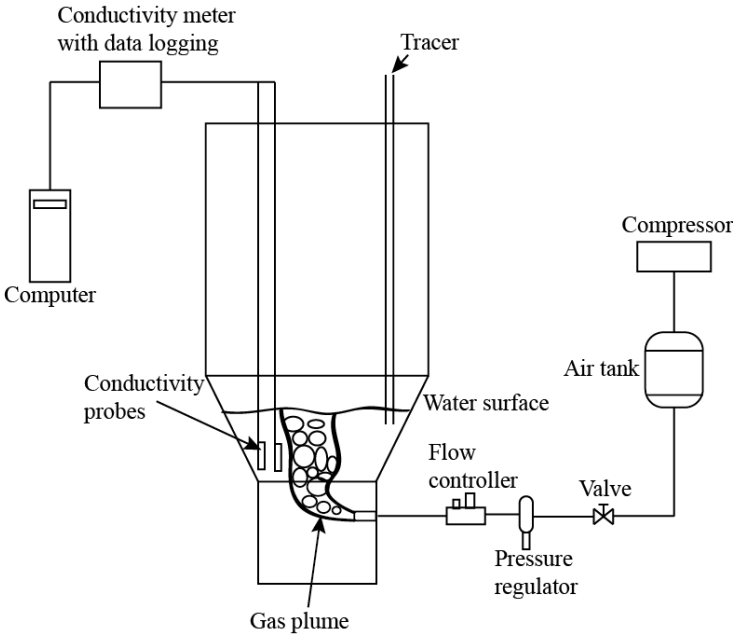

Figure 2: Schematic picture of the physical mixing time water experiments.

Table 1. Parameters used in the physical water model experiments and in the real process.

Parameters	Physical water model	Real process
Scale	1:3	1
Flow rate (Nm^3h^{-1})	17	265
Bath height liquid (m)	0.37	1.1
Nozzle height location (m)	0.145	0.435
Density liquid (kgm^{-3})	998.2	3562
Density gas (kgm^{-3})	1.226	0.1887
Diameter of cylinders (m)	0.433 / 0.2	1.3 / 0.6
Diameter tuyere (m)	0.0117	0.035

3. Numerical model

The Eulerian multiphase model was used to describe the interface between the injected gas and the liquid [21]. A species transport model was used to describe the tracer movement in the bath of the reactor. Furthermore, the tracer concentration was monitored at two different measurement points in the liquid bath.

3.1. Boundary conditions and solution methods: validation case (water)

The boundary conditions of the numerical model correspond to the experimental setup, which are given in table 1. Air was injected into the water through the nozzle. The speed of the air at the inlet of the nozzle was approximately 44 ms^{-1} (Mach 0.13), when accounting for the measured and controlled gas flow rate and diameter of the nozzle. The flow was assumed to be incompressible due to the low Mach number of 0.13, based on previous experience from the pilot plant trials. In the mathematical model, the volume fraction of air at the inlet exit was set to 1 and a mass flow inlet was used as boundary condition for the gas injection. Also, a pressure outlet with a pressure condition equal to atmospheric pressure was used at the top of the domain, i.e. the top part of the reactor. The walls were treated as stationary walls having a no-slip condition and standard wall functions were used.

A 3D hexahedral mesh was used (in most parts of the domain). One of the main functions with this mesh is the large number of hex cells. Specifically, three different meshes were tested for the sensitivity of the domain, namely coarse (17000), medium (44000) and fine (111000). The simulations were run in transient mode, due to the turbulent flow in the bath which was clearly visible in the experimental setup. The tracer was patched into the domain and was added into the bath after 30 seconds of stirring. Specifically, this time represents a time several times longer than the measured mixing time. In this way, it was ensured that the bath had reached a fully developed flow before a tracer was added. The pressure velocity coupling was solved with the spatial discretization the least square cell-based method. Also, a constant time step of 0.0001 was used throughout the entire simulation.

3.2. Boundary condition and solution methods, IRONARC case

The boundary conditions were partly similar as used in a previous paper [3]. The domain for the IronArc gas-slag mixing time simulation can be seen in figure 3. The injected gas, which consists of an air over LPG ratio equal to approximately 20, was assumed to have the properties of air at the elevated temperature of 1600 °C. Thus, it was assumed that the gas obtained the slag temperature momentarily. Also, the slag was assumed to completely consist of FeO. The simulations were performed under isothermal conditions, which means the gas and slag properties represent the properties at 1600°C. Furthermore, the gas density was calculated by using the ideal gas law and a constant value was used during the entire simulation. Also, the flow was assumed to be incompressible, due to the fact that the inlet velocity of the gas at the operating temperature was 450 ms^{-1}. This is below 1 Mach at the operating temperature conditions. The tracer in this case had the same properties as the slag and it was patched at the same location(approximately) where the tracers were added in the water model experiments. Similarly, the measurement points in the gas-slag simulation were the same as the location of the probes in the water model experiment.

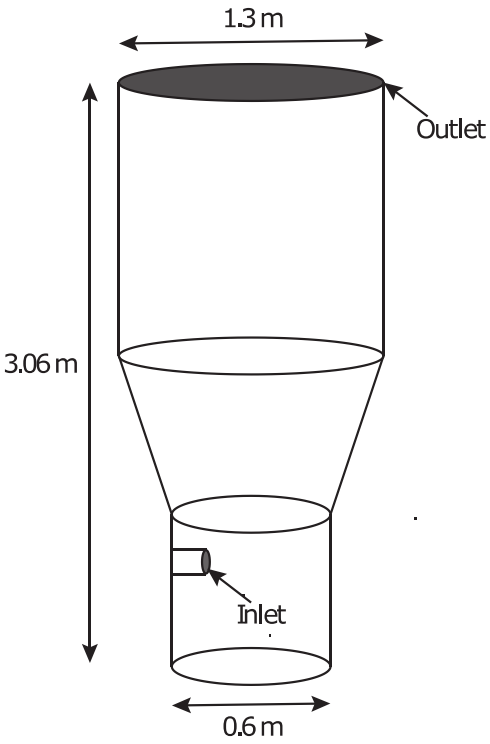

Figure 3: Domain of the IronArc simulation, including inlet, outlet and dimensions.

3.3. Theory

3.3.2. Eulerian Multiphase model

For the Eulerian multiphase model, the different phases are treated as interpenetrating continua and a set of equations are solved for each phase. Both phases are treated as continuous media and are averaged over each control volume. Furthermore, both the continuity and momentum equations are solved for each phase and a single pressure is shared between the phases. The momentum transfer between the gas and water is modeled by using a drag term. A diameter is set for the secondary phase, which in this case is the dispersed gas bubble. Also, the turbulence is calculated per phase and both phases are considered to be incompressible.

In the Eulerian multiphase model, the continuity equation for the Eulerian multiphase model reads as follows:

$$\frac{1}{\boldsymbol{\rho_{rq}}}\left(\frac{\partial}{\partial t}\left(\boldsymbol{\alpha_q \rho_q}\right) + \nabla \cdot \left(\boldsymbol{\alpha_q \rho_q \overline{v}_q}\right) = \sum_{p=1}^{n}\left(\dot{m}_{pq} - \dot{m}_{qp}\right)\right) \quad (2)$$

where $\bar{\boldsymbol{v}}_{\boldsymbol{q}}$ is the velocity of phase $\boldsymbol{q}$ and $\dot{m}_{pq}$represents the mass transfer from the p^{th} to q^{th} phase, and $\dot{m}_{qp}$represents the mass transfer from phase $\boldsymbol{q}$ to phase $\boldsymbol{p}$. Also, $\boldsymbol{\alpha}_{\boldsymbol{q}}$ is the volume fraction of phase q and $\boldsymbol{\rho}_{\boldsymbol{q}}$ is the density of the qth phase. The parameter $\boldsymbol{\rho}_{\boldsymbol{rq}}$ is the volume averaged density of the qth phase in the solution domain.

The momentum equation for phase q is expressed as follows:

$$\begin{aligned}\frac{\partial}{\partial t}\left(\boldsymbol{\alpha}_{\boldsymbol{q}}\boldsymbol{\rho}_{\boldsymbol{q}}\bar{\boldsymbol{v}}_{\boldsymbol{q}}\right) + \nabla\cdot\left(\boldsymbol{\alpha}_{\boldsymbol{q}}\boldsymbol{\rho}_{\boldsymbol{q}}\bar{\boldsymbol{v}}_{\boldsymbol{q}}\bar{\boldsymbol{v}}_{\boldsymbol{q}}\right) \\ = -\boldsymbol{\alpha}_{\boldsymbol{q}}\nabla p + \nabla\cdot\bar{\bar{\boldsymbol{\tau}}}_{\boldsymbol{q}} + \boldsymbol{\alpha}_{\boldsymbol{q}}\boldsymbol{\rho}_{\boldsymbol{q}}\bar{\boldsymbol{g}} \\ + \sum_{p=1}^{n}\left(K_{\boldsymbol{pq}}(\bar{\boldsymbol{v}}_p - \bar{\boldsymbol{v}}_q) + \dot{m}_{pq}\bar{\boldsymbol{v}}_{pq} - \dot{m}_{qp}\bar{\boldsymbol{v}}_{qp}\right) + \bar{\boldsymbol{F}}_{\boldsymbol{q}}\end{aligned} \tag{3}$$

where $\bar{\bar{\boldsymbol{\tau}}}_{\boldsymbol{q}}$the q: th phase stress strain tensor, Fq is an external body force between the different phases,. $\bar{\boldsymbol{v}}_{pq}$ is the interphase velocity, and $\bar{\boldsymbol{g}}$ is the gravitational acceleration constant. The parameter K_{pq} is an exchange coefficient between the phases and p is the pressure shared by the phases. The general form of the K_{pq} is defined as follows:

$$K_{\boldsymbol{pg}} = \frac{\rho_p f}{6\tau_p} d_p A_i \tag{4}$$

where $\rho_p$is the density of phase p, $\tau_p$is the particulate relaxation time, A_i the interfacial area, and f is the drag function. The latter drag function is defined as follows:

$$f = \frac{C_D Re}{24} \tag{5}$$

where Re is the Reynolds number and C_D is the drag coefficient. In this case, the drag coefficient from the Schiller Naumann Model is used [21-23].

3.3.3 Turbulence Theory

The Realizable k-ε model was used to describe the turbulence in the domain:

The turbulent viscosity is calculated by combining k and e and is defined as follows:

$$\mu_t = C_\mu \frac{k^2}{\varepsilon} \tag{6}$$

The transport equations for k and ε are defined as follows:

$$\frac{\partial(\rho k)}{\partial t} + \frac{\partial(\rho k u_j)}{\partial x_j} = \frac{\partial}{\partial x_j}\left[\left(\mu + \frac{\mu_t}{\sigma_k}\right)\frac{\partial k}{\partial x_j}\right] + G_k + G_b - \rho\varepsilon - Y_M + S_k \tag{7}$$

and

$$\frac{\partial(\rho\varepsilon)}{\partial t} + \frac{\partial(\rho\varepsilon u_j)}{\partial x_j} = \frac{\partial}{\partial x_j}\left[\left(\mu + \frac{\mu_t}{\sigma_k}\right)\frac{\partial \varepsilon}{\partial x_j}\right] + \rho C_1 S\varepsilon - \rho C_2 \frac{\varepsilon^2}{k + \sqrt{v\varepsilon}} + C_{1\varepsilon}\frac{\varepsilon}{k} C_{3\varepsilon} G_b + S_\varepsilon \tag{8}$$

where Gk is the production of turbulent kinetic energy due to mean velocity gradients, which is defined as follows:

$$G_k = -\rho\overline{u_i' u_j'}\frac{\partial u_j}{\partial x_i} \tag{9}$$

3.3.4 Species Transport Model

The mixing, and in turn the mixing time, in the bath of the process reactor was calculated by using the species transport model. The following equations were solved for the species transport model in the bath:

$$\frac{\partial(\rho Y)}{\partial t} + \nabla \cdot \rho\overline{\boldsymbol{v}}\, Y = -\nabla \cdot \bar{J}$$

where Y is the mass fraction of species and J is the diffusion flux of species. Also, for turbulent flows the diffusion is calculated as follows:

$$\bar{J} = -\left(\rho D_m + \frac{\mu_t}{SC_t}\right)\nabla \cdot Y$$

where Dm is the mass diffusion coefficient for species SC_t is the turbulent Schmidt number, μ_t is the turbulent viscosity.

4. Results and discussion

4.1 Validation case, water model

The mixing time was predicted using mathematical modeling. Thereafter, the numerical model results were compared to physical model results. The mixing time curves that show the tracer concentration over time can be seen in figure 4. Figures 4a) and b) show the curves for the numerical predictions and figures 4c) and d) show the curves from the water model experiment. In both the numerical and experimental cases, the tracer concentration increases fast after a tracer addition. Thereafter, the curves reach a peak value before them evens out at a value of unity (1) after only seconds. However, the curves are a bit different in appearance. For the numerical results (Fig.4 a)) the peak concentration is approximately 3.5 times the final value while for the experimental (Fig.4c)) case the peak only reaches just above 1.1. This difference in concentration curve appearance is due to the tracer addition in the different cases. For the water model experiments, the tracers were poured into the water. This convection makes the tracer content at the probe position to be more diluted compared to the numerical model simulations. Specifically, the tracer in the numerical model was patched into the domain as a spherical shape. Hence, a larger amount of tracer will be positioned at the probe location and in turn there will be a higher peak for the numerically predicted curves. However, the curves for both the numerical model evens out fast and both show similar mixing times. For the physical water model experiments the average mixing times where 7.6 s and 10.2 s for a 95% and a 99% homogenization degree respectively: this under the condition that one inlet and a flow rate of 282 $NLmin^{-1}$ was used. The average predicted mixing time was found to be 7.5 seconds. The difference between the predicted and measured mixing time results was 1.3%, which means that the numerical model results are in good agreement with the physical model results in terms of predicting the mixing behavior.

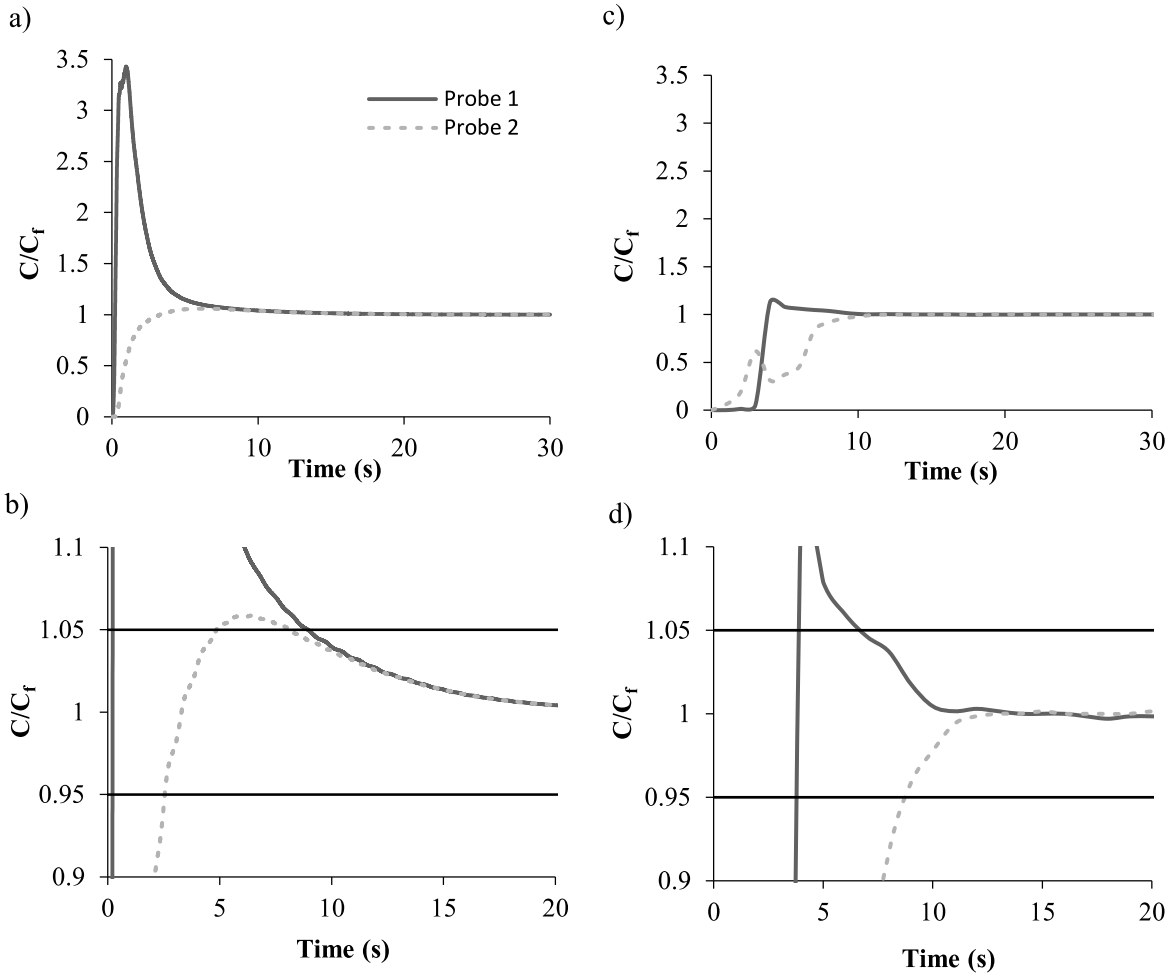

Figure 4: Tracer concentration curves as a function of time for both predictions a) and b) and experiments c) and d)

4.2 IRONARC pilot plant (simulation only)

The mixing time in the pilot plant and the tracer concentration curves can be seen in Figure 5. It is similar to the results from the water model simulation in the sense that the point of measurement close to the tracer increases to above 2 times the final concentration, while the other measurement point does not increase to the same level. However, both curves reach within the positions of lines 1.05 and 0.95, which a represents a 95% homogenization degree in the bath. This simulation predicted a mixing time of 6.5 seconds for a 95% homogenization degree. This is a mixing time that is below 10 seconds. These results are in line with the mixing time results from the earlier investigation, were the mixing times were determined in pilot plant trials [4]. These results are close agreement to the downscaled water model simulations as well as the water model experiment results.

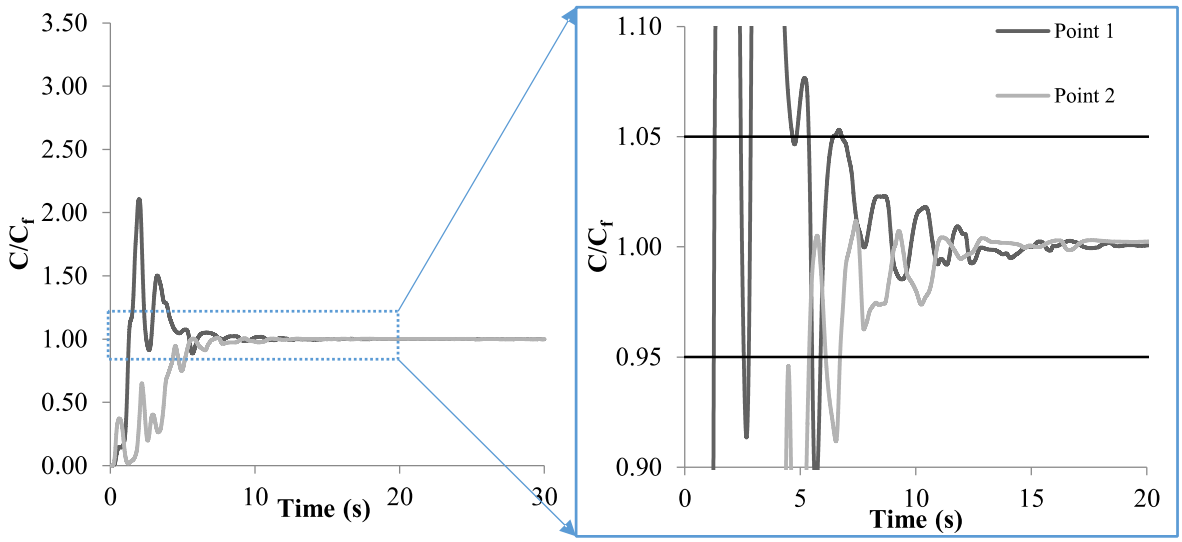

Figure 5: Tracer concentration curves for the pilot plant slag simulation.

The wall shear stress on the pilot plant reactor wall was predicted and the results are shown in figure 6a)-f). This figure shows the shear stress of a maximum of 30 Pa, to be able to clearly see which areas on the walls that are mostly affected after 30 seconds of gas injection. The maximum shear stress value was seen in the tuyere region. Other areas that had high wall shear stress values were located at the opposing wall of the tuyere, as is clearly seen in figures 6a) to 6f). This area is located at the same height level as the tuyere and hence at the same level as the injected gas. The penetration depth of the gas injection in this process was determined in a previous study [3]. The results showed that the penetration depth was approximately 30 cm and hence the gas reaches to the center of the reactor. According to these results, the opposing wall of the injected gas is affected by higher shear stresses even though the gas does not reach the wall. Moreover, the gas creates a flow, which will push the slag against that wall which will create a high shear stress. This is in line with the observed refractory wear during operation of this pilot plant process, which according to our experience had been seen after trials at approximately the same locations as these shear stress graphs shows.

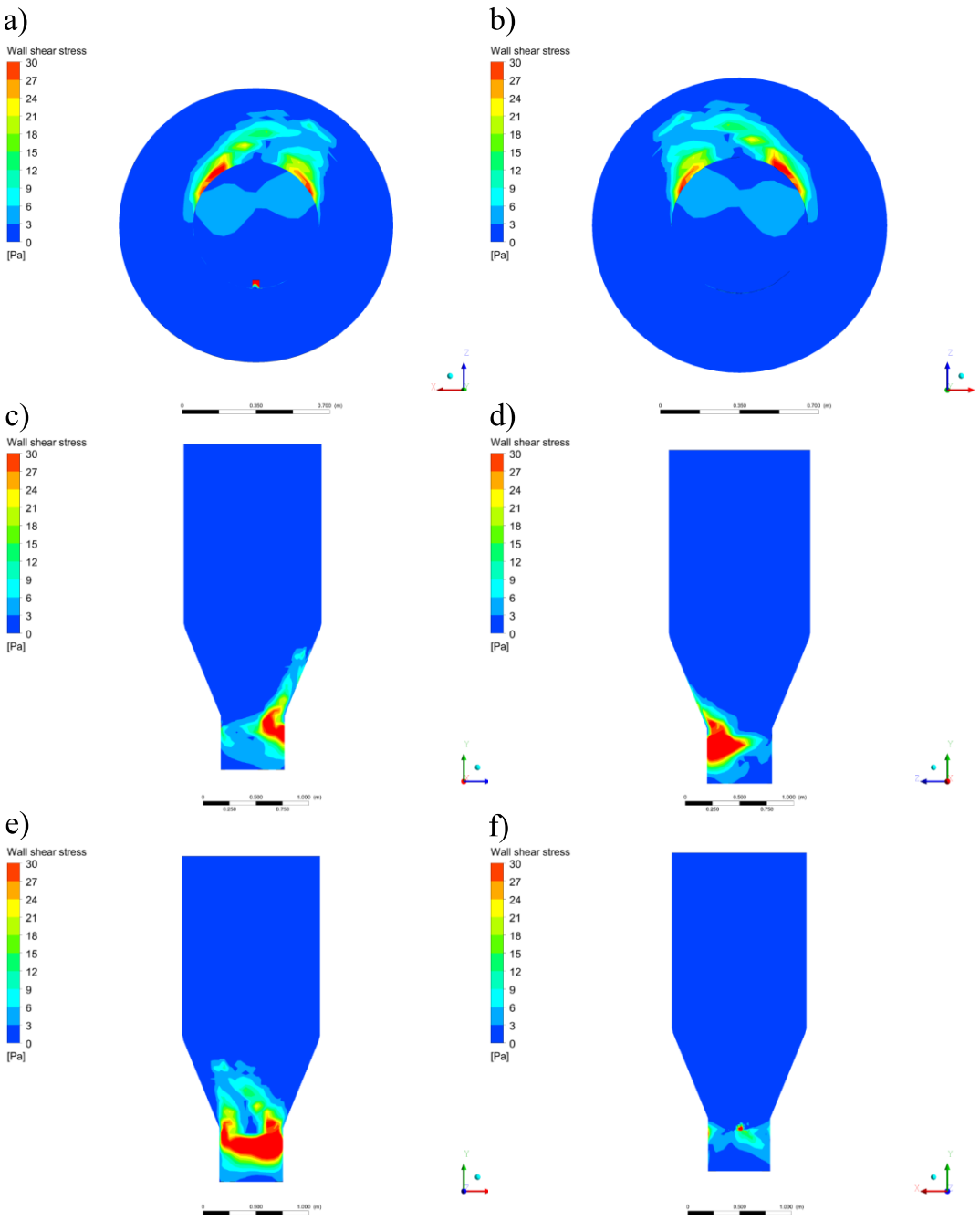

Figure 6: The shear stress on the wall of the pilot plant with the maximum shear stress of 30 Pa. It is shown from a) above, b) below, c) right side, d) left side, e) opposite side of the nozzle locations, and f) nozzle wall.

The velocity vector flow fields at four different planes are illustrated in figure 7.

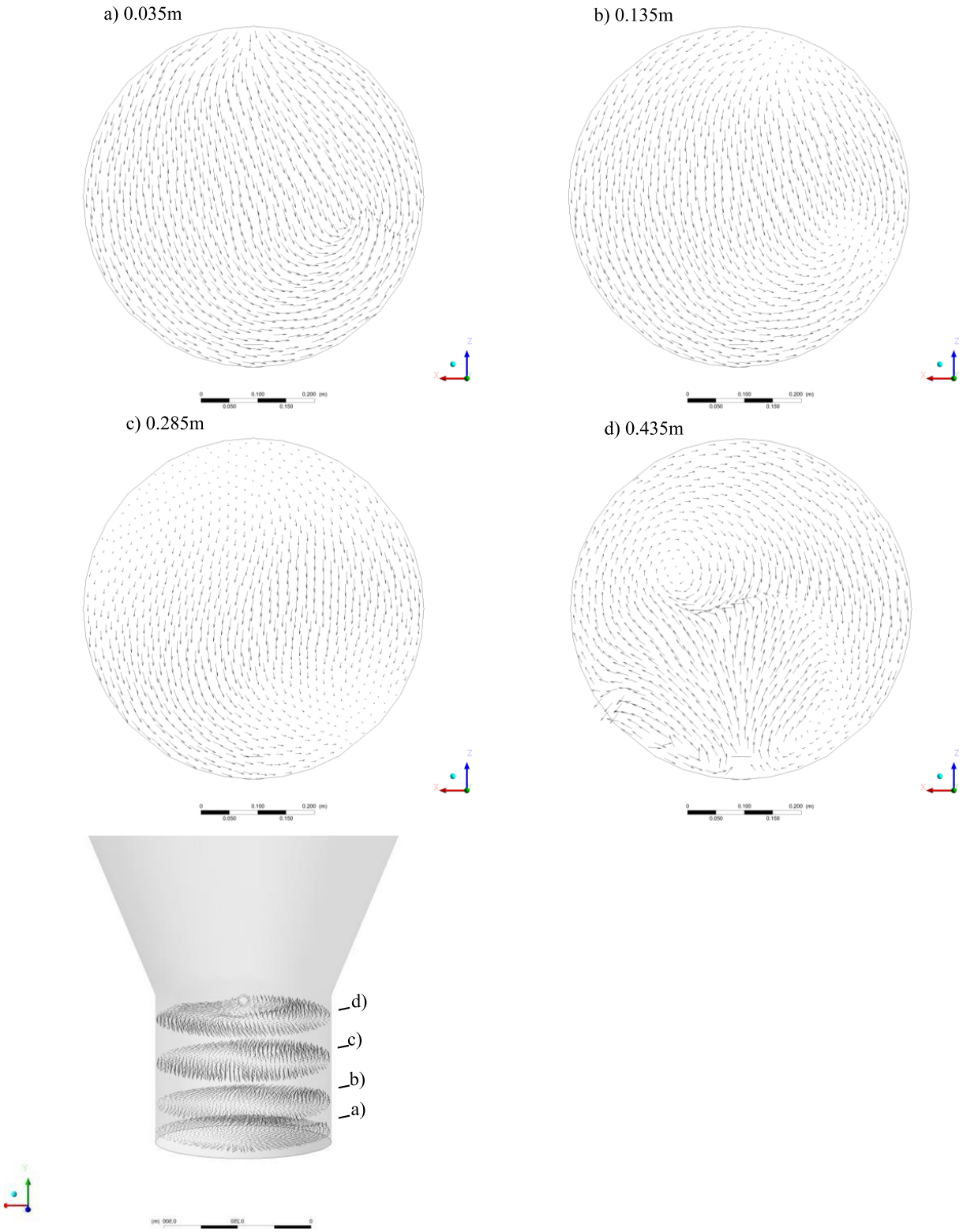

Figure 7: Slag velocity vector arrows for different planes located in the bottom part of the pilot plant reactor domain. a) a plane 0.035 m from the bottom, b) a plane 0.135 from the bottom, c) a plane 0.285 m from the bottom and d) a plane 0.435 m from the bottom.

5. Conclusions

The mixing time has been determined for the newly developed IronArc process, based on mathematical modeling. First physical water model experiments were performed in a 1/3 scale acrylic plastic model. The mixing times were determined by measuring the tracer concentration at two different positions in the water bath over time. A 95% homogenization degree was chosen as the homogenization degree to be obtained at the measuring points. In addition, the mixing times were also predicted numerically, with a setup that corresponded to the experimental setup. The mixing time in the IronArc pilot plant was also predicted by using the same numerical model as was used to predict the mixing time for the smaller water model. Overall, the following specific conclusions can be drawn based on the results from this investigation:

- The mixing time for the physical experiments were determined to be 7.6 seconds, based on the averaging the mixing time for 6 trials performed to reach a 95% homogenization degree This result is valid for one inlet and a flow rate of 282 $NLmin^{-1}$. The mixing time for the numerical model was 7.5 seconds, which corresponds to a 1.3% difference compared to the experimental mixing times. Specifically, this means that the numerical model results are in good agreement with the physical model results in terms of predicting the mixing behavior.
- The predicted mixing time was 6.5 seconds in the hot pilot scale simulation, which is slightly faster than the water model mixing time. Specifically, the difference in mixing time is less than one second. In addition, these results are in line with the mixing time results determined through industrial trials which showed that the mixing times were less than 10 seconds.
- The maximum shear stress was found at a location close to the tuyere and the second highest values were found at the area on the opposite wall to the nozzle. This may cause a higher wear on the lining in these areas.
- The numerical model can be used in further simulations where the upscaling of the IronArc process is investigated.

Acknowledgements

The author wishes to thank Jernkontoret and the Axel Ax:son Johnsson research fund for the financial support that enabled to finish this article. Also, the author would like to thank ScanArc Plasma Technologies in Hofors, Sweden.

References

[1] S. Santen, M. Imris (ScanArc Plasma Technologies AB) *SE 536 291 C2*, **2013**.

[2] K. Bölke, M. Ersson, P. Ni, M. Swartling, P.G. Jönsson: Steel Res. Int. **2018**, vol. 89, pp. 1-10.

[3] K. Bölke, M. Ersson, M. Imris, P.G. Jönsson: ISIJ Int. **2018**, vol. 58, 1210-17.

[4] K.Bölke, N. Andersson, M. Ersson, P.G. Jönsson, Experimental Determinations of Mixing Times in the IronArc Pilot Plant Process. *Metals* **2019**, 9, 101.

[5] V. Visuri, E. Isohookana, A. Kärnä, T. Haas, R.H. Eriç, T. Fabritius, 5th Int. Conf. on Process Development in Iron and Steelmaking, Luleå Sweden, June **2016**.

[6] P. Samuelsson, P. Ternstedt, A. Tilliander, A. Apell, P. G. Jönsson, *Ironmak. Steelmak.* **2016**, 1.

[7] P. Ternstedt, A. Tilliander, P. G. Jönsson, M. Iguchi, *ISIJ int.* **2010**, 50, 663.

[8] C. Wupperman, N. Giesselmann, A. Rückert, H. Pfeifer, H. Odenthal, *ISIJ Int.* **2012**, 52, 1817.

[9] J. H. Wei, J. C. Ma, Y. Y. Fan, N. W. Yu, S. L. Yang, S. H. Xiang, D. P. Zhu, *Ironmak. Steelmak.***1999**, 26, 363.

[10] J. H. Wei, *Journ. of Shanghai Univers.* **2002**, 6, 1

[11] T. M. J. Fabritius, P. T. Mure, J.J Harkki, *ISIJ Int.* **2003**, 43, 1177.

[12] H. J. Odenthal, U. Thiedemann, U. Falkenreck, J. Schlueter, *Metall. Trans. B* **2010**, 41, 396.

[13] T. M. J. Fabritius, P. A. Kupari, J. J. Harkki, *Scand. Journ. of Metall.* **2001**, 30, 57

[14] J. H. Wei, H. L. Zhu, H. B. Chi, H. J. Wang, *ISIJ Int.* **2010**, 50, 26.

[15] X. Zhou, M. Ersson, L. Zhong, J. Yu, P. G. Jönsson, *Steel Res. Int.* **2014**, 85, 273.

[16] Y. Li, W. T. Lou, M. Y. Zhu; *Ironmak. Steelmak.* **2013**, 40, 505-514.

[17] D.K. Chibwe, G. Akdogan, C. Aldrich, R. H. Eric, Chemical product and process modeling. **2011**, 6, 1-28

[18] A. Tilliander, T. L. I. Jonsson, P. G. Jönsson, *ISIJ Int.* **2004**, 44, 326.

[19] X. Zhou, M. Ersson, L. Zhong, J. Yu, P. G. Jönsson, *ISIJ Int.* **2014**, 54, 2255.

[20] X. Zhou, M. Ersson, L. Zhong, J. Yu, P. G. Jönsson, *Steel Res. Int.* **2015**, 85, 1.

[21] ANSYS 15.0 Fluent Theory Guide, ANSYS Inc., USA (**2013**)

[22] F. Kerdouss, A. Bannari and P. Proulx: *Chem. Engin. Sci.* 61(**2006**), 3313.

[23] P. Chen, J. Sanyal and M.P. Dudukovic: *Chem. Engin. Sci*, 59(**2004**), 5201